■ 445

Assessment of Early Hypertensive Retinopathy using Fractal Analysis of Retinal Fundus Image

Wiharto*, Esti Suryani, Muhammad Y. Kipti
Department of Informatics, Sebelas Maret University
Jl. Ir. Sutami No. 36A, Surakarta, Indonesia
*Corresponding author, e-mail: wiharto@staff.uns.ac.id

Abstract

 Hypertensive retinopathy is characterized by changes in retinal vessels, a change known as tortuosity. Automated analysis of retinal vascular changes will make it easier for clinicians to make an initial diagnosis of the disease. The pattern of blood vessels in the retina of the eye can be approached with a fractal pattern. This study proposes a method for the early detection of disease hypertensive retinopathy using the fractal analysis approach fundus retinal image. Variable fractal used is the fractal dimension and lacunarity, whereas for the classification algorithm using ensemble Random Forest and validation using the k-fold cross-validation. Performance measurement using the parameters of accuracy, positive prediction value (PPV), negative prediction value (NPV), sensitivity, specificity and area under the curve (AUC). The test results using 10-fold cross-validation values obtained accuracy 88.0%, PPV 84.0%, NPV 92.0%, sensitivity 91.3%, specificity 85.19%, and 88.25% AUC. The performance is produced when using lacunarity the box size 2^2. Based on the research results, it can be concluded that early detection of hypertensive retinopathy with fractal analysis approaches have a performance based on AUC produced included in good categories.

Keywords: hypertensive retinopathy, fractal analysis, retinal, tortuosity, classification

1. Introduction

 Hypertension is a global health problem that requires attention. It can lead to death both in developed countries or developing countries. A survey conducted by the World Health Organization (WHO) in 2000, showed the number of people worldwide suffers from hypertension approximately 26.6% for men and 26.1% for women. It is estimated by 2025 the number will increase to 29.2% [1]. Hypertension, if not handled properly could cause complications of health problems, one of which is the change of retinal vascularization, commonly called hypertensive retinopathy. Changes in retinal vascularization can also indicate blood vessel abnormalities of the brain, heart, and kidneys [2]. Examination of retinal vessels can be done by using a fundus camera. A complete analysis of the results of the examination should be performed by an ophthalmologist. This makes the problem, because many areas that have not been reached by ophthalmologists, so the process of diagnosis will have difficulty. The automated computer-based retinal analysis will be of great help to clinicians at the primary service level, thus being able to be used as a support for early detection of hypertensive retinopathy.

 Hypertensive retinopathy disease according to Keith-Wagener-Barker (1939), classified into 4 stages. Stage I, one of the characteristics is the tortuosity of retinal arterioles. Stage II has the characteristics of definite narrowing of blood vessels. Stage III with one of the characteristics of retinopathy (cotton-wool spots, arteriosclerosis, hemorrhagic). Stage IV is one of the characteristics is edema neuroretinal including papilledema, Siegrist line, elschnig spot. Based on the classification, characteristics of early disease hypertensive retinopathy is the tortuosity of arterioles. Tortuosity is a picture of retinal blood vessels tortuous. Changes in retinal vascular tortuosity in the form retinal arterioles or veins are tortuous, resulting in a change in the pattern of retinal blood vessels.

 The development of research on hypertensive retinopathy disease diagnosis concentrated in making a diagnosis in stage II. In stage II is characterized by the constriction of blood vessels. The constriction can be measured by calculating the ratio of artery-vein (AVR).

Research by Narasimhan et.al[3], proposed the model of hypertensive retinopathy diagnosis by performing segmentation of retinal blood vessels, and then estimate the width ratio artery-vein blood vessels (AVR). The result of the comparison is obtained, for hypertensive retinopathy within the range of 0.24 to 0.49, while for the normal 0.6 - 0.7. A similar study conducted by Noronha et.al [4], in this study a comparison of normal AVR if the value is more than 2/3, while hypertensive retinopathy, if less than 2/3. Manikis et.al [5], also proposes a framework for diagnosis of hypertensive retinopathy disease with hessian-based segmentation of blood vessels, then calculate the value of the AVR as a sign of the disease. A number of similar studies, ie, performed a diagnosis of hypertensive retinopathy using AVR parameters such as those performed by Ortiz et.al [6], Khitran et.al [7], Triwijoyo et.al [8], Faheem et.al[9] and Muramatsu et.al [10].

The next model of the diagnostic system is based on the texture of retinal fundus imagery, as did Triwijoyo et.al [11]. The research is resized the image, then converted into CSF format and classified with Convolutional Neural Network. Texture analysis, particularly for analyzing retinal vessels, may also be performed using fractals. Fractal analysis has several variables including the fractal dimension and lacunarity. The fractal dimension can be used to determine the relationship of changes in retinal blood vessels of mortality caused by coronary heart disease [12]. The study was supported by research conducted Zhu et.al [13]. The study explains that the fractal dimension retinal images have a relationship with blood pressure and central retinal arteriolar equivalent (CRAE) so that the fractal dimension can also be used as an indicator of cardiovascular risk [13].

The use of fractal dimensions was also used by Cavallari et al. [14], the study performed retinal blood vessel analysis for the diagnosis of hypertensive retinopathy. Parameters used, while the fractal dimension also used tortuosity index, in the study grouped the fractal dimension and tortuosity index values by using k-mean clustering. In the fractal analysis to describe the characteristics of a fractal of the same dimensions with different textures is done by using Lacunarity [15]. Thus, lacunarity complete the fractal dimension that only can know how many places are populated with data. Lacunarity used for calculation of the distribution of the degree of emptiness (lacunas) in the image. This is evidenced in a study conducted by Talu et.al [16] which determined the global assessment retinal vascular network for amblyopia patients. The results showed lacunarity parameters for amblyopia retinal image is smaller compared to the normal retinal image.

Based on a number of studies that have been done before, in this study developed a system for prior assessment of hypertensive retinopathy disease using fractal analysis. The fractal analysis used is the fractal dimension and lacunarity. The algorithm used to classify positive or negative hypertensive retinopathy is a random forest algorithm. The parameters of performance used are sensitivity, specificity, accuracy, PPV, NPV, and area under the curve (AUC) [17].

2. Research Method
2.1 Data
This study uses data from the retinal image dataset STARE. The dataset can be obtained by accessing online via URL http://www.ces.clemson.edu/~ahoover/stare/. STARE project was built and started in 1975 by Michael Goldbaum, MD at the University of California, San Diego. STARE funded by the US National Institutes of Health. During its history, more than 30 people who contributed to the project STARE. Images and clinical data provided by the Shiley Eye Center at the University of California, San Diego, and the Veterans Administration Medical Centered San Diego. The data obtained has been divided into two retinal images. They are healthy (normal) and hypertensive retinopathy (abnormal). The data used to be 50 images, which consisted of 25 healthy retinal images and 25 images hypertensive retinopathy.

2.2 Fractal
Fractals are derived from the Latin fractus meaning broken or irregular. Basically, a fractal is a simple geometry that can be broken up into several parts that have a shape like the previous form with a smaller size [15]. Fractals have the properties of self-similarity, self-affinity, self-inverse, and self-squaring. The nature of self-similarity indicates that consists of fractal shaped parts similar to each other. Self-affinity illustrate that fractal composed of parts mutually

intertwined with each other. Self-inverse means a part of a fractal can be an inverted arrangement of another arrangement, while the self-squaring means that a portion of the fractal is an increase in complexity of the previous section[18]. Fractals are all forms that have similarities with itself [15].

2.3 Fractal Dimension

Fractals have different dimensions to the dimensions of objects in everyday life which are the dimension Euclid space, ie 1, 2, and 3. Values dimensional objects on Euclid be an integer, such as a 1-dimensional line for long, because the field of dimension 2 has a length and width, while the pick-dimensional space 3 for length, width, and depth. One method for calculating the fractal dimension of an image is Box Counting method [19]. The method can be expressed in an equation, as shown in Equation (1). The concept of this method is to divide the image into a grid of smaller ones with a certain size.

$$D = \frac{\log(N)}{\log(1/r)} \tag{1}$$

where N is the number of boxes containing objects, D fractal dimension of the object, and r is the ratio. The steps of the method of calculating fractal dimension Box Counting method according to Backes & Bruno [20] are as follows:

a. The image is divided into squares with a size r, r value changed from 1 to 2k, with k = 0, 1, 2, ..., and 2k can't be larger than the size of the image. When the image size is 2m x 2m then the value of k will stop until m.
b. N count the number of boxes containing the parts object in the image. The value of N depends on r.
c. Calculating the value $\log(1/r)$ and $\log(N)$.
d. Make a straight line using a value $\log(1/r)$ and $\log(N)$.
e. Calculating the slope of the straight line with Equation (2). The slope value is the fractal dimension of the image based on the Equation (3).

$$\propto = \frac{(\sum_{k=1}^{n} xy) - \frac{(\sum_{k=1}^{n} x)(\sum_{k=1}^{n} y)}{n}}{(\sum_{k=1}^{n} x^2) - \frac{(\sum_{k=1}^{n} x)^2}{n}} \tag{2}$$

$$FD = -\propto \tag{3}$$

with α is the slope value, n much data is used, x is the value $\log(1/r)$, y is the value $\log(N)$, and FD is the value of the fractal dimension.

2.4 Lacunarity

Lacunarity is a special term in geometry. It is referring to the pattern measurement method, especially fractals, fill space, where patterns having a gap of more or larger generally have lacunarity greater value [21]. The method for calculating lacunarity first introduced in general by Mandelbort [15], and a lot of algorithms that can be used to calculate the value lacunarity an image. The algorithm is the most commonly used method is Gliding box introduced by Allain and Cloitre [22] and popularized by Plotnick et al [23].

Steps Gliding Box algorithm begins by placing a box or square box with the image size r x r in the upper left corner of the image. The next step will be to check the box of each pixel containing a 1 or 0 until finally the whole pixels is exceeded by the box. The box is moved from the top left corner past the image pixel by pixel of the image until the entire pixel in the image is identified. When the box is at a particular pixel, the program will calculate each pixel value which passed is considered as objects in the image. The frequency of content distribution obtained pixels in each box is denoted by n(M,r). The frequencies will be used to determine Q(M,r) as the probability distribution of each value in the box. Q(M,r) obtained by dividing the distribution per pixel with a maximum total amount of the course of these boxes is denoted by N(r). Furthermore, the distribution will be processed by the following formula:

$$Z(1) = \sum MQ(M, r) \tag{4}$$

$$Z(2) = \sum M^2 Q(M, r) \tag{5}$$

From both the above Equations obtained the lacunarity formula to calculate the size of the box are, Λ (r) as follows:

$$\Lambda(r) = \frac{Z(2) - (Z(1))^2}{(Z(1))^2} \tag{6}$$

2.5 Random Forest Algorithm

The random Forest algorithm is an improvement of the CART algorithm. Repairs carried out by applying the bootstrap method of aggregating (bagging) and Random feature selection [24]. In the data set consisting of m observations and explanatory variables p, then the stages in the Random Forest algorithm can be described as follows [24]:

1. Stages bootstrap: Perform a random sampling with size m with recovery on cluster training data.
2. Stages feature random selection: stacking tree based on these data to the maximum size without pruning. At each node, the selection of the sorting is done by selecting random explanatory variables m, where m << p. M the best sorter selected from the explanatory variables.
3. Repeat steps 1-2 as many times in order to obtain k random tree
4. Make a prediction by using a combination of a number k of the tree fruits (eg, using a majority vote for the classification of cases, or average for cases of regression)

2.6 Method

The research method is divided into several stages, as shown in Figure 2. The first stage, the process of data collection which used are using datasets STARE. The second stage is the fundus retinal image segmentation. The segmentation phase consists of several processes as shown in Figure 3. In Figure. 3 can be explained that the fundus camera image acquisition results in the form of color images, then steps must be done is the gray-scale process to obtain the gray level image. Grayscale an image has four types, namely ordinary gray-scale, red channel, the green channel and blue channels. Four types of gray scale of the image of the green channel have the best reflection of light, so it can produce good information about the structure of the blood vessels and the retina [25]. After the subprocess green channel, then the process CLAHE (Contrast Limited Adaptive Histogram Equalization), this process serves to homogenize the spread of the retinal image histogram, to obtain images with good contrast.
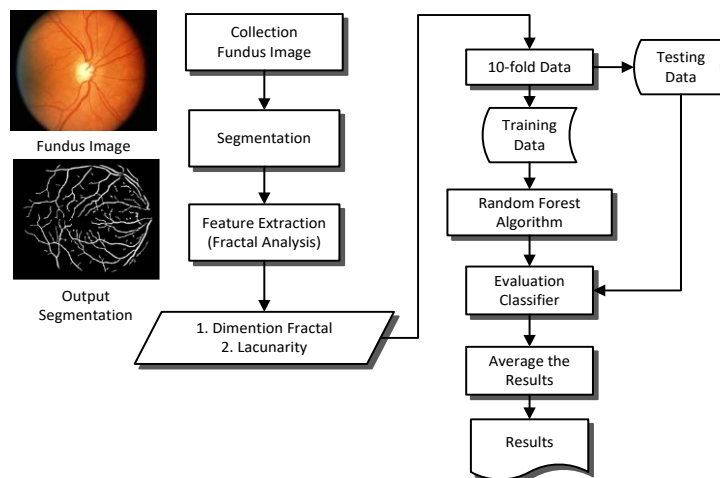

Figure 2. Research Method

Average filtering process using a filter to remove noise, background exclusion process is then performed. The process uses subtract operation CLAHE image with the image of the filter to eliminate variations in the background image of the retina. The next process is the process of thresholding, namely to transform into a binary image. After the threshing process will obtain a binary image of blood vessels of the retina, but there are other objects that form the edge of the retina [25]. Retinal image masking is required to eliminate edge retinal image [26]. Masking the image of the retina obtained by changing the image of the retinal fundus color to grayscale images first. After that, it will check the value of each pixel. If the pixel value is more than the prescribed limit, it will be changed to 255 or white color. Conversely, if the pixel value is less than the prescribed limit, then it will be converted to 0 or black. The last step is done a post-filtration process, the process of removing the edge of the retina using thresholding the image of the subtracts operation, with image masking retina. So we get the binary image of the retinal blood vessels form background color to black and white color to the blood vessels of the retina.
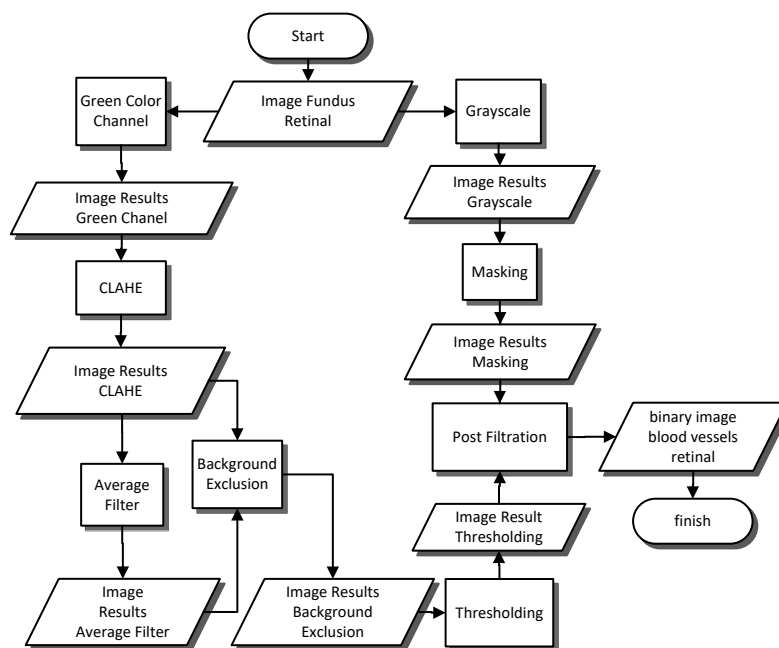

Figure 3. Image Segmentation

The next stage is the feature extraction, segmentation results of the image, which is a binary image of the retinal blood vessels. The process of feature extraction is done with fractal analysis to get the fractal dimension using a box counting method and lacunarity using gliding box. The process is shown in Figure. 4. The next stage is classification. Classification is done using the algorithm in classification RandomForest. The output stages of feature extraction and lacunarity form fractal dimension of a number of input images become RandomForest classification algorithm. Stages of the latter are to perform testing and analysis of system performance. The method used for testing is k-fold cross-validation with k = 10. In such method is done by dividing the data into k groups at random, then use k-1 group for training and one group for testing. The process is repeated so k the group once used for testing. The resulting performance is the average of the tests.

Performance analysis is performed using the Confusion matrix calculation, as shown in Table 1. The performance parameters are analyzed is accuracy, PPV, NPV, specificity, sensitivity, and AUC. The performance parameters are calculated based on the formula shown in equation (7-12). Interpretation of the performance parameters especially AUC has two approaches, namely statistically and clinically. In this study uses only one clinical variable, namely retinal vein tortuosity, the approaches used to interpret the AUC values using statistical approaches.

$$PPV = \frac{TP}{TP+FP} \tag{7}$$

$$NPV = \frac{TN}{TN+FN} \tag{8}$$

$$Sensitivity = TP_{rate} = \frac{TP}{TP + FN} \tag{9}$$

$$Specificity = TN_{rate} = \frac{TN}{TN+FP} \tag{10}$$

$$Accuracy = \frac{TP+TN}{TP+TN+FP+FN} \tag{11}$$
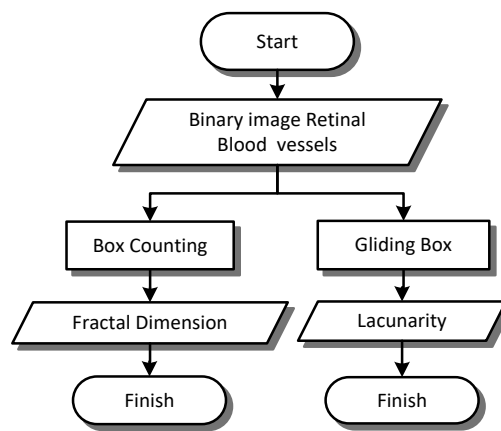
$$AUC = \frac{1+TP_{rate}-(1-TN_{rate})}{2} \; [27] \tag{12}$$
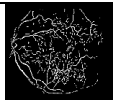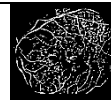
Figure. 4. Feature Extraction Retinal Blood Vessels
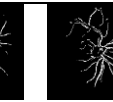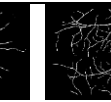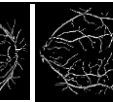
Table 1. Confusion Matric

Actual Class	Predictive Class	
	Positive	Negative
Positive	TP (True Posiitive)	FN (False Negative)
Negative	FP (False Positive)	TN (True Negative)

3. Results and Analysis

The result of the process of feature extraction using fractal analysis of binary image segmentation results can be shown in Table 2. The table shows some sample dimension value fractal and lacunarity, for the positive and negative image of hypertensive retinopathy. It also indicated the sample stage retinal image segmentation results, both negative positive and hypertensive retinopathy. Testing for feature lacunarity done using various sizes box. Size box used in the calculation lacunarity, with the Gliding-box algorithm is $2^1, 2^2, 2^3, \ldots, 2^9$.

Table 2. Sample of Results Feature Extraction with Fractal Analysis

		Hypertensive Retinopathy				Normal		
Image									
FD		1.5827	1.6349	1.6516	1.5304	1.4484	1.5247	1.5082	1.4302
L	2^1	6.4665	4.9875	4.5008	8.8571	11.034	9.0509	8.1649	10.1949
a	2^2	4.9351	3.8732	3.5149	7.0244	9.0095	6.7333	6.4779	8.5226
c	2^3	3.0335	2.4143	2.2353	4.6053	6.1535	4.0804	4.2654	5.9469
u	2^4	1.4666	1.1185	1.0581	2.3548	3.3759	2.0762	2.1751	3.2241
n	2^5	0.6649	0.5466	0.5116	1.1536	1.7863	1.0300	0.9792	1.5624
a	2^6	0.2826	0.2635	0.2583	0.5806	1.0063	0.5104	0.4217	0.7874
r	2^7	0.1009	0.0911	0.1105	0.2470	0.4901	0.2186	0.1394	0.3915
i	2^8	0.0088	0.0161	0.0316	0.0479	0.1643	0.0966	0.0131	0.1581
t	2^9	0.0015	0.0007	0.0022	0.0063	0.0013	0.0069	0.0011	0.0044
y									

Referring to the data in Table 2, performed significance test to determine the difference between the dimensions fractal and lacunarity on positive or negative condition hypertensive retinopathy. Tests carried out using the t-test, using a confidence level of 95%. These values have the understanding that, if the t-test showed a p-value <0.05, then feature fractal dimension and lacunarity have significant differences in normal and hypertensive retinopathy retina. Detailed test results are shown in Table 3.

The results of significance testing, as shown in Table 3, that the fractal dimension between normal with hypertensive retinopathy significantly different (p-value <0.05). It was confirmed that changes sharply in the arch that affect the retinal blood vessels fractal dimensional changes. This is reinforced in research Zhu et al [13], which explains that the fractal dimension associated with blood pressure and cardiovascular risk factors. Blood pressure (hypertension) acute is the major cause hypertensive retinopathy. Fractal dimension values for normal conditions is smaller compared with hypertensive retinopathy.

Table 3. The Results of Significance Test

Feature	Mean±STD		p-value
	Normal	Retinopathy	
Fractal Dimension	1.4878±0.0422	1.5221±0.0437	0.000069
Lacunarity 2^1	9.7316±1.8923	7.8785±2.0538	0.002126
Lacunarity 2^2	7.7295±1.5441	6.1441±1.5638	0.001350
Lacunarity 2^3	5.1057±1.1253	3.9495±1.0248	0.000959
Lacunarity 2^4	2.7291±0.7181	2.0214±0.5764	0.000739
Lacunarity 2^5	1.3906±0.4642	1.0089±0.3190	0.001761
Lacunarity 2^6	0.7252±0.3297	0.5170±0.2020	0.008010
Lacunarity 2^7	0.337±0.2173	0.2193±0.1115	0.015628
Lacunarity 2^8	0.1105±0.0923	0.0553±0.0413	0.007708
Lacunarity 2^9	0.0037±0.0050	0.0027±0.0024	0.172182

The next stage is the result of classification to determine the positive or negative hypertensive retinopathy. Classification is done by using the Random Forest algorithm. The classification process is done by using some of the features that combined with fractal dimension, lacunarity size variation box. Performance parameters used is based upon the parameters used in the medical world. These parameters are sensitivity, specificity, PPV, NPV, AUC [17] and accuracy. The process of training and testing is performed using the k-fold cross-validation with the value of k = 10. The results of performance measurement methods 10-fold cross validation as shown in Table 4

Table 4 Performance of Diagnosis System

Feature	Sencitivity	Specificity	PPV	NPV	Accuracy	AUC
FD	0.8400	0,8400	0.8400	0.8400	0.8400	0.8400
FD+lac1	0.8750	0.8462	0.8400	0.8800	0.8600	0.8606
FD+lac2	**0.9130**	**0.8519**	**0.8400**	**0.9200**	**0.8800**	**0.8825**
FD+lac3	0.8400	0.8400	0.8400	0.8400	0.8400	0.8400
FD+lac4	0.5000	05000	0.1600	0.8400	0.5000	0.5000
FD+lac5	0.7600	0.7600	0.7600	0.7600	0.7600	0.7600
FD+lac6	0.7692	0.7917	0.8000	0.7600	0.7800	0.7804
FD+lac7	0.8000	0.8000	0.8000	0.8000	0.8000	0.8000
FD+lac8	0.7407	0.7826	0.8000	0.7200	0.7600	0.7617
FD+lac9	0.8261	0.7778	0.7600	0.8400	0.8000	0.8019

Feature lacunarity, referring to the results of the significance test, showed significant differences between normal and hypertensive retinopathy. This difference applies to all sizes of box used in the calculation lacunarity, except for the size of the box 2^9. Values lacunarity produced, normally has a greater value than the hypertensive retinopathy. The condition is the same as the value generated in research Talu et.al[16], which explains the value lacunarity for patients with amblyopia has a value that is smaller than normal.

Classification by exploiting a feature in the form of fractal dimension deliver the performance, for all the performance parameters worth 84.00%. Referring to the AUC values then the system performance by using these features shows that the system provides performance in good categories [28]. Merging feature lacunarity combination with fractal dimension, to the size of the box 2^4 to 2^9, providing the performance is still below the performance if the classification is done simply using fractal dimension. By the time the size of the box 2^3, the performance of the system generated the same as when using only the feature fractal dimension. The combination of fractal dimension feature with lacunarity with the size of the box 2^1 and 2^2 provide improved performance for the parameters AUC of 2.06% and 4.24%. The combination of fractal dimension with size lacunarity box 2^2 provides the best system performance, with a value of 88.25% AUC. Referring interpretation AUC values statistically, then the system performance diagnosis included in a good category.

The model of the early detection system of proposed hypertensive retinopathy has better performance compared with a number of studies using AVR parameters, as shown in Table 5. The proposed model is included in the early screening category, or early detection, when referring to Dahlan's study [17] then the main performance parameters are sensitivity. Referring to the parameter of sensitivity, the proposed model is relatively good compared to a number of existing studies, except with studies conducted by Khitran et.al [7]. The difference in performance with the research of Khitran et.al [7], is possible due to the difference of dataset so that the characteristics of each tested data are different. These differences result in the resulting performance difference. The proposed system model, when viewed from the performance parameters of the combination of sensitivity and specificity, ie AUC, the proposed system is relatively better than some previous studies.

Table 5. Comparison with a Number of Previous Studies

Authors	Dataset	Sensitivity	Specificity	AUC
Manikis et.al[5]	STARE	0.7189	0.9656	0.8423
Mendoca & Campilho[29]	STARE	0.6999	0.9569	0.8284
Soeres et.al [30]	STARE	0.7103	0.9737	0.8420
Staal et.al [31]	STARE	0.6970	0.9810	0.8390
Khitran et.al[7]	DRIVE	0.9700	0.9900	0.9800
	VICAVR	0.9600	0.9800	0.9700
Proposed	**STARE**	**0.9130**	**0.8519**	**0.8825**

4. Conclusion

Based on this research, some conclusions can be drawn. First, feature extraction results obtained, the retinal image of hypertensive retinopathy diagnosed had an average of fractal dimension is higher than the normal retinal image and lacunarity lower. The second

merger fractal dimension and lacunarity able to deliver improved system performance diagnosis than just using fractal dimension. Third best box size of lacunarity capable of giving their best performance was 2^2. Finally, the proposed system is capable of delivering performance in either category, with the values of sensitivity 91.30% specificity 85.19%, accuracy 88.0%, PPV 84.0%, NPV 92.0%, and 88.25% AUC.

References

[1] R. E. A. Apriany and T. Mulyanti. Protein, Saturated Fat, Sodium, Fiber Intake and BMI(Body Mass Index) are Related with Blood Pressure Hypertension Patient in Tugurejo Hospital Semarang, Semarang: Diponegoro University; 2012.

[2] S. Setyowati and Lestariningsih. Factors that have a role to the Hypertensive Retinopathy incidence in Non-Diabetic Essential Hypertension Patient, Semarang: Diponegoro University; 2005.

[3] K. Narasimhan, V. C. Neha, and K. Vijayarekha. *Hypertensive Retinopathy Diagnosis from Fundus Images by Estimation of AVR*. in International Conference on Modeling Optimization and Computing (ICMOC-2012). India. 2012; 38: 980–993.

[4] K. Noronha, K. T. Navya, and K. P. Nayak. *Support system for the automated detection of hypertensive retinopathy using fundus images*. in International Conference on Electronic Design and Signal Processing (ICEDSP). India. 2012: 7–11.

[5] G. C. Manikis *et al.. An image analysis framework for the early assessment of hypertensive retinopathy signs*. in E-Health and Bioengineering Conference (EHB). Romania. 2011: 1–6.

[6] D. Ortiz *et al.. System Development for Measuring the Arterious Venous Rate (AVR) for the Diagnosis of Hypertensive Retinopathy*. 2012 IV Andean Region International Conference (ANDESCON). Cuenca, Ecuador. 2012: 53–56.

[7] S. Khitran, M. U. Akram, A. Usman, and U. Yasin. *Automated system for the detection of hypertensive retinopathy*. in 4th International Conference on Image Processing Theory, Tools and Applications (IPTA). Paris, France. 2014: 1–6.

[8] B. K. Triwijoyo and Y. D. Pradipto. Detection of Hypertension Retinopathy Using Deep Learning and Boltzmann Machines. *J. Phys. Conf. Ser.*, 2017; 801(1): 1-7.

[9] M. R. Faheem and Mui-zzud-Din. Diagnosing Hypertensive Retinopathy through Retinal Images, *Biomed. Res. Ther.*, 2015, 2(10): 385-388.

[10] C. Muramatsu, Y. Hatanaka, T. Iwase, T. Hara, and H. Fujita. Automated selection of major arteries and veins for measurement of arteriolar-to-venular diameter ratio on retinal fundus images. *Comput. Med. Imaging Graph.*, 2011, 35(6): 472–480.

[11] B. K. Triwijoyo, W. Budiharto, and E. Abdurachman. *The Classification of Hypertensive Retinopathy using Convolutional Neural Network*. 2nd International Conference on Computer Science and Computational Intelligence. Bali, Indonesia. 2017; 116: 166–173.

[12] G. Liew *et al..* Fractal analysis of retinal microvasculature and coronary heart disease mortality, *Eur. Heart J.*, 2011; 32(4): 422–429.

[13] P. Zhu *et al..* The Relationship of Retinal Vessel Diameters and Fractal Dimensions with Blood Pressure and Cardiovascular Risk Factors, *PLoS ONE*, 2014; 9(9): 1-10.

[14] M. Cavallari, C. Stamile, R. Umeton, F. Calimeri, and F. Orzi. Novel Method for Automated Analysis of Retinal Images: Results in Subjects with Hypertensive Retinopathy and CADASIL, *BioMed Res. Int.*, 2015; 2015: 1–10.

[15] B. B. Mandelbrot. *The Fractal Geometry of Nature*. New York: W. H. Freeman and Company, 1982.

[16] S. Talu, C. Vlăduţiu, L. A. Popescu, C. A. Lupaşcu, Ş. C. Vesa, and S. D. Ţălu. Fractal and lacunarity analysis of human retinal vessel arborisation in normal and amblyopic eyes, *Hum. Vet. Med.*, 2013; 5(2): 45–50.

[17] M. S. Dahlan. *Diagnostic Research: Theoretical Basics and Applications with SPSS and Stata Programs.* Jakarta: Salemba Medika, 2009.

[18] H. O. Peitgen, H. Jürgens, and D. Saupe. *Fractals for the classroom. Part 1.: Introduction to fractals and chaos*. New York: Springer-Verlag, 1992.

[19] W. Li, P. Fu, and E. Zhang. Application of fractal dimensions and fuzzy clustering to tool wear monitoring, *Indones. J. Electr. Eng. Comput. Sci.*, 2013; 11(1): 187–194.

[20] A. R. Backes and O. M. Bruno. *A new approach to estimate fractal dimension of texture images*, in International Conference on Image and Signal Processing, Cherbourg-Octeville, France. 2008: 136–143.

[21] T. G. Smith, G. D. Lange, and W. B. Marks. Fractal methods and results in cellular morphology-dimensions, lacunarity and multifractals, *J. Neurosci. Methods*, 1996; 69(2): 123–136.

[22] C. Allain and M. Cloitre. Characterizing the lacunarity of random and deterministic fractal sets, *Phys Rev*, 1991; 44(6): 3552–3558.

[23] R. E. Plotnick, R. H. Gardner, and R. V. O'Neill. Lacunarity indices as measures of landscape texture, *Landsc. Ecol.*, 1993; 8(3): 201–211.

[24] L. Breiman. "Random Forests," *Mach. Learn.*, 2001; 45(1): 5–32.

[25] R. A. Aras, T. Lestari, H. A. Nugroho, and I. Ardiyanto. Segmentation of retinal blood vessels for detection of diabetic retinopathy: A review, *Commun. Sci. Technol.*, 2016; 1(1): 33-41.

[26] I. Jamal, M. U. Akram, and A. Tariq. Retinal image preprocessing: background and noise segmentation, *TELKOMNIKA Telecommun. Comput. Electron. Control*, 2012; 10(3): 537–544.

[27] E. Ramentol, Y. Caballero, R. Bello, and F. Herrera. SMOTE-RSB *: a hybrid preprocessing approach based on oversampling and undersampling for high imbalanced data-sets using SMOTE and rough sets theory, *Knowl. Inf. Syst.*, 2012; 33(2): 245–265.

[28] F. Gorunescu. Data Mining Concepts,Models and Techniques, Intelligent Systems Reference Library. Berlin, Heidelberg: Springer, 2011.

[29] A. M. Mendonca and A. Campilho. Segmentation of retinal blood vessels by combining the detection of centerlines and morphological reconstruction, *IEEE Trans. Med. Imaging*, 2006; 25(9): 1200–1213.

[30] J. V. B. Soares, J. J. G. Leandro, R. M. Cesar, H. F. Jelinek, and M. J. Cree, Retinal vessel segmentation using the 2-D Gabor wavelet and supervised classification, *IEEE Trans. Med. Imaging*, 2006; 25(9): 1214–1222.

[31] J. Staal, M. D. Abramoff, M. Niemeijer, M. A. Viergever, and B. van Ginneken. Ridge-Based Vessel Segmentation in Color Images of the Retina, *IEEE Trans. Med. Imaging*, 2004; 23(4): 501–509.